

Computational Methods in Plasma Physics

Sara R.J. Wilson
University of Pittsburgh
Email: srw81@pitt.edu

Abstract

Plasma is a state of matter that results from a gas having undergone ionization that plays a fundamental role in both natural and technological systems. Mathematically speaking, plasmas are governed by magnetohydrodynamic (MHD) equations. This paper provides an expository overview of the ideal MHD equations and the numerical schemes often used to approximate their solutions. I conclude with a discussion of future studies.

1 Introduction

A wide range of technologies and scientific processes rely on plasmas, including fusion devices, jet propulsion systems (Figure 1), and solar flares. Because of this, it is important that these systems are modeled as accurately as possible. Adequately understanding these systems typically requires an MHD framework, which models the interaction fluid and electromagnetic behaviors. In this paper, I provide an overview of the MHD equations and two popular choices of numerical methods used to approximate their solutions.

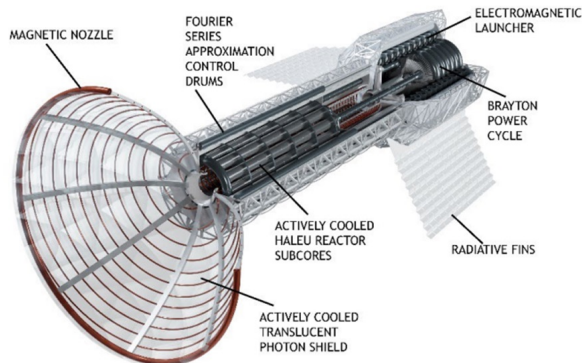


Figure 1: NASA Proposed Pulsed Plasma Rocket (PPR) [1]

The exposition in Sections 2 through 5 of this paper is adapted from [2], which served as the primary reference for this project. In this paper, I consider the ideal MHD equations in

particular. Numerical methods, such as finite difference methods and finite element methods, and their applicability to various MHD systems, will be discussed. The finite element method will be examined in the context of eigenvalue problems. Lastly, I present my proposed future research directions.

2 Ideal MHD Equations

There are numerous ways to formulate an MHD system. In particular, the ideal MHD equations are derived from the resistive MHD equations. This model is a limiting case of the two-fluid MHD and treats the electrons and ions as a single fluid with a unified pressure. To obtain the ideal MHD formulation, we first non-dimensionalize these equations using the Alfvén velocity, the Alfvén time , and the time over which resistive effects are most important which are given by

$$\begin{aligned} V_A &= \frac{B}{\sqrt{\mu_0 n M_i}} \\ \tau_A &= \frac{a}{V_A} \\ \tau_R &= \frac{\mu_0 a^2}{\eta} \end{aligned}$$

The terms relating to resistivity are multiplied by the inverse magnetic Lundquist number $S^{-1} \equiv \frac{\tau_R}{\tau_A}$. Alfvén waves propagate along magnetic field lines, carrying energy and momentum. Such waves are damped by resistive effects, so if we only care about fast time scales, we can neglect these terms. Thus, we obtain a very rich system, the ideal MHD equations.

$$\frac{\partial \rho}{\partial t} + \nabla \cdot \rho \mathbf{u} = 0 \quad (1)$$

$$\nabla \times (\mathbf{u} \times \mathbf{B}) = \frac{\partial \mathbf{B}}{\partial t} \quad (2)$$

$$\rho \left(\frac{\partial \mathbf{u}}{\partial t} + \mathbf{u} \cdot \nabla \mathbf{u} \right) + \nabla p = \mathbf{J} \times \mathbf{B} \quad (3)$$

$$\frac{\partial p}{\partial t} + \mathbf{u} \cdot \nabla p + \gamma p \nabla \cdot \mathbf{u} = 0 \quad (4)$$

with (1) the continuity equation, (2) the induction equation, (3) the equation of motion, and (4) the equation of state. Note $\mathbf{u} :=$ velocity, $p :=$ pressure, $\mathbf{B} :=$ magnetic field, $\rho :=$ fluid density, $\mathbf{J} :=$ current density, and $\frac{5}{3} = \gamma :=$ ratio of specific heats. Note that non-dissipative macroscopic solutions are fundamentally unchanged.

3 Finite Difference Method

In this section, a brief overview of finite differences is provided. We seek to find an approximation for the derivative. Recall the Taylor expansion

$$f(x+h) = f(x) + f'(x)h + \frac{f''(x)h^2}{2} + \dots + \frac{f^{(n)}(x)h^n}{n!} + o(h^n)$$

Neglecting the higher-order terms, it is clear that $f'(x) \approx \frac{f(x+h)-f(x)}{h}$, and this approximation is first-order accurate. This is precisely how we obtain finite difference methods. However, we instead write this using index notation. Consider the forward Euler method for an ordinary differential equation as a simple example. Begin by introducing a uniform grid on the interval $[a, b]$. Let the grid points be defined by

$$x_i = a + ih, \quad i = 0, 1, \dots, N,$$

where the grid spacing is

$$h = \frac{b-a}{N}.$$

We denote by u_i the approximation to $u(x_i)$. Using this notation, the forward finite difference approximation of the first derivative at x_i is

$$u'(x_i) \approx \frac{u_{i+1} - u_i}{h}.$$

This formula is obtained by replacing the derivative with the difference quotient over one grid-step in the positive direction. As a related example, the forward difference for an ODE $u'(t) = F(t, u)$ uses this same idea, giving the update $u_{i+1} = u_i + h F(t_i, u_i)$. In addition to the forward difference, there are two other basic finite difference formulas. The backward difference is written as

$$u'(x_i) \approx \frac{u_i - u_{i-1}}{h},$$

which simply replaces the forward step with a backward step and uses values from the left. Not all schemes are created equal, some are higher accuracy. For example, we have the central difference

$$u'(x_i) \approx \frac{u_{i+1} - u_{i-1}}{2h},$$

which is obtained by combining the Taylor expansions about x_i in both directions. This provides a second-order accurate approximation.

Finite differences are also used to approximate higher order derivatives. For example, the standard second derivative is given by

$$u''(x_i) \approx \frac{u_{i+1} - 2u_i + u_{i-1}}{h^2}.$$

This expression is obtained by adding the Taylor expansions for $u(x+h)$ and $u(x-h)$ and isolating the second derivative term. Finite differences provide a large slate of options, thus

are widely applicable across problems. For example, finite difference time domain (FDTD), or Yee's method, is often used with Maxwell's equations. FDTD is a finite difference method which is second order accurate in both space and time that uses a staggered spatial grid and leapfrog time marching. Essentially, this means that values of the electric field "live" on the cell edges while values of the magnetic field "live" on the center, with the time stepping of each misaligned with each other.

4 Finite Element Method

Similarly, finite elements approximate a vector space. In particular, they combine the Galerkin approximation with the selection of a discrete subspace. Although finite elements are often more reliable for complex problems than finite differences, they are also more computationally tasking. It is important to note that accuracy alone does not fully characterize the quality of a method. Stability must also be considered, especially when approximations are used in partial differential equations. A method may be consistent, but it may still produce unreliable results if it is not stable. It is important to ensure that the physics of the problem is retained, so accuracy, stability, and computational cost must be considered jointly.

Here, we outline the Galerkin method. First, we must convert our problem into the desired form. Essentially, we follow this game plan: Select a test function in a Hilbert space containing the weak solution, say $\varphi \in X$, multiply φ through the equation, then integrate. Utilizing multivariate integration by parts allows us to push derivatives from the partial differential equation to the test functions. This allows us to obtain a variational, or weak, formulation of the problem. This gives us a problem of the following form

$$a(u, \varphi) = \mathcal{F}(\varphi) \quad \forall \varphi \in X$$

with $a(u, \varphi)$ a continuous and coercive bilinear form and \mathcal{F} some bounded linear functional.

Now we may proceed with the Galerkin approximation. Take some $X^h \subset X$ and get

$$a(u^h, \varphi^h) = \mathcal{F}(\varphi^h) \quad \forall \varphi^h \in X^h$$

There is much to be said, and much more work to be done, concerning the stability and error of finite element methods. Here we will present two results concerning convergence and stability

Lemma 1 (Cea). *Suppose $a(\cdot, \cdot) : X \times X \rightarrow R$ is a continuous and coercive bilinear form and $\mathcal{F} : X \rightarrow R$ is a bounded linear functional. Let $X^h \subset X$ be a finite dimensional subspace of X . Then, there is a unique $u^h \in X^h$ satisfying*

$$a(u^h, \varphi^h) = \mathcal{F}(\varphi^h) \quad \forall \varphi^h \in X^h$$

The error $u - u^h$ satisfies

$$\|u - u^h\|_X \leq \left(1 + \frac{a_1}{a_0}\right) \inf_{\varphi^h \in X^h} \|u - \varphi^h\|_X$$

with a_0, a_1 constants obtained via coercivity and continuity, respectively.

Lemma 2 (Ladyzhenskaya-Babuška-Brezzi (LBB)). *Let X denote the velocity space and Q the pressure space arising in the mixed formulation of an incompressible flow problem. The pair (X^h, Q^h) is said to satisfy the Ladyzhenskaya-Babuška-Brezzi (LBB) condition if there exists a $\beta > 0$ such that*

$$\inf_{q^h \in Q^h} \sup_{\mathbf{v}^h \in X^h} \frac{(\nabla \cdot \mathbf{v}^h, q^h)}{\|\mathbf{v}^h\|_X \|q^h\|_Q} \geq \beta.$$

The LBB condition provides a stability criterion for pressure. For an example, we briefly mention one classical finite element pair, the Hood-Taylor elements

$$X^h = \left\{ v \in [C^0(\Omega)]^d : v|_T \in [\mathcal{P}_2(T)]^d \quad \forall T \in \mathcal{T}_h \right\}$$

$$Q^h = \left\{ q \in C^0(\Omega) : q|_T \in \mathcal{P}_1(T) \quad \forall T \in \mathcal{T}_h \right\}.$$

These elements provide an explicit construction of the discrete spaces X^h suitable for approximation of the Navier-Stokes equations. This is useful for describing the fluid behavior of a plasma volume. Note the velocity is approximated by continuous piecewise quadratic functions, while the pressure is approximated by continuous piecewise linear functions. This choice satisfies the LBB condition, and thus provides a reliable pair of spaces. Although there is much more nuance in implementation, this highlights how abstract frameworks translate to concrete applications in modeling real physical systems.

5 Eigenvalue Problem

5.1 Formulation

One use of finite elements is to tackle problems of the form

$$\mathcal{L}(U) = \lambda U$$

with \mathcal{L} the self-adjoint operator, λ the scalar eigenvalue, and U the unknown. We multiply some test function $\varphi^h \in X^h$ through the above problem and integrate. If we use the expansion $U = \sum_{j=1}^N a_j \psi_j^h$ with $\psi_1^h(x), \dots, \psi_N^h(x)$ a basis of X^h . we end up with the Galerkin formulation of the problem.

5.2 Plasma Column

With the mathematics of finite elements established, it is interesting to see how they operate in a real plasma configuration. A plasma column is a high-aspect ratio toroidal plasma surrounded by vacuum and a conducting wall . This example illustrates how the abstract finite element ideas introduced earlier translate into the matrices and eigenvalue problems used in practical plasma modeling. These have many uses, from fusion devices to science museum exhibits (Figure 2).



Figure 2: Plasma Column Exhibit at the Technorama Swiss Science Center [3]

Oftentimes in modeling physical systems, we end up with nonphysical numerical artifacts. For example, spectral pollution occurs when spurious eigenvalues which are not actual eigenvalues of the problem are produced. We seek to minimize this. The equations for the displacement and magnetic vector potential of the plasma in a spectral pollution minimizing torus are

$$\begin{aligned}\xi &= R^2 \nabla U \times \nabla \phi + \omega R^2 \nabla \phi + R^{-2} \nabla_{\perp} \chi \\ \mathbf{A} &= R^2 \nabla \phi \times \nabla f + \psi \nabla \phi - F_0 \ln R \hat{Z}\end{aligned}$$

The associated eigenvalue problem is

$$\omega^2 \mathbf{A} \cdot \mathbf{x} = \mathbf{B} \cdot \mathbf{x}$$

where

$$\begin{aligned}A_{ij} &= \rho_0 \int_0^a r dr \phi'_i \phi'_j + \rho_0 m^2 \int_0^a \frac{1}{r} dr \phi_i \phi_j \\ B_{ij} &= \int_0^a r dr (F \phi_i)' (F \phi_j)' + m^2 \int_0^a \frac{1}{r} dr F^2 \phi_i \phi_j + m F^2 \left[\frac{1 + (a/b)^{2m}}{1 - (a/b)^{2m}} \right] \delta_{NN} \\ \mathbf{x} &= [a_0, a_1, \dots, a_N]\end{aligned}$$

This eigenvalue system is obtained after projecting the governing equations onto a chosen set of basis functions, so the matrices \mathbf{A} and \mathbf{B} arise naturally as finite element stiffness and mass matrices. In this sense, the problem of ideal plasma column stability fits directly into the finite element framework introduced earlier in the paper.

6 Potential Research

In this section, I present my proposed research in [4]. Tokamaks, a machine that utilizes magnetic fields to confine plasmas in a torus for thermonuclear fusion, are often modeled using coupled magnetohydrodynamic (MHD) and kinetic equations to capture both macroscopic and microscopic behavior. The MHD-kinetic equations are

$$\frac{\partial n_s}{\partial t} + \nabla \cdot (n_s \mathbf{V}_s) = 0 \quad (5)$$

$$\frac{\partial(m_s n_s \mathbf{V}_s)}{\partial t} + \nabla \cdot \boldsymbol{\pi}_s = n_s \langle \mathbf{F}_s \rangle \quad (6)$$

$$\frac{1}{2} m_s \frac{\partial}{\partial t} (n_s \langle v_s^2 \rangle) + \nabla \cdot \left(\frac{n_s m_s}{2} \langle v_s^2 \rangle \right) = n_s \langle \mathbf{F}_s \cdot \mathbf{v}_s \rangle \quad (7)$$

Due to the dependence on spatial scaling, it is essential to accurately simulate the spatial scale-switch in modeling the MHD-kinetic equations. If this is not handled appropriately, there will be abrupt, nonphysical jumps in the solution of the system. Consequently, numerical methods for the MHD-kinetic equations have frequent occurrences of shocks and spurious oscillations, leading to destabilization in the solution. To avoid this, many solvers use discontinuous Galerkin (DG) methods. These pose issues with computation, as they couple local solutions through their shared boundaries. In contrast, Hybridized discontinuous Galerkin (HDG) methods express solutions in terms of approximate traces on the boundaries. However, HDG lacks the shock capturing that DG has.

Shock capturing methods with HDG have been investigated [5], but the implementation is not robust largely due to not being weakly divergence-free (div-free) in the magnetic field. This would account for the conservation of magnetic flux, as required by Gauss' Law for magnetism which states that $\nabla \cdot \mathbf{B}$. Physically this means that there are no magnetic monopoles, and the magnetic field lines form closed, continuous loops. An open question I aim to answer is identifying a scale switching indicator between the MHD and kinetic portions. While existing hybrid methods rely on heuristic switchers, I predict that a theoretical error bound derived from the div-free HDG formulation can be utilized.

My proposed work will focus on deriving a div-free HDG formulation and testing such an indicator. In particular, I seek to use $H(\text{div})$ -conforming elements. To establish the notion of $H(\text{div})$ -conforming elements, consider the following definitions and lemma presented in [6].

Definition 1. Let \mathcal{T}_h be a triangulation of Ω . Let \mathcal{E}_h be the set of open edges of the finite element mesh. Define the set of boundary edges as

$$\mathcal{E}_h^B := \{e \in \mathcal{E}_h : e \cap \partial\Omega \neq \emptyset\}.$$

The set of interior edges is then

$$\mathcal{E}_h^I := \mathcal{E}_h \setminus \mathcal{E}_h^B.$$

Definition 2. If for $\mathbf{w} \in L^p(\Omega)$ with $p \geq 1$ there exists $\rho \in L^1_{loc}(\Omega)$ such that the distributional divergence can be represented in the form

$$-\int_{\Omega} \nabla \psi \cdot \mathbf{w} dx = \int_{\Omega} \psi \rho dx \quad \forall \psi \in C_0^\infty(\Omega),$$

then the function $\rho := \nabla \cdot \mathbf{w}$ is called the weak divergence of \mathbf{w} .

This prepares us for the following essential lemma.

Lemma 3. Let \mathbf{W}_h denote the space of piecewise polynomials with respect to the partition \mathcal{T}_h . Then $\mathbf{W}_h \subset H(\text{div}, \Omega)$, provided the normal components of functions in this space are continuous across all inter-element boundaries $e \in \mathcal{E}_h^I$.

Here, an outline of the proof is presented.

Proof. Let $\mathbf{w}_h \in \mathbf{W}_h$ and suppose the normal component of \mathbf{w}_h is continuous across each $e \in \mathcal{E}_h^I$. Define $\rho_h \in L^2(\Omega)$ by setting

$$\rho_h|_T = (\nabla \cdot \mathbf{w}_h)|_T, \quad \forall T \in \mathcal{T}_h.$$

Using the divergence theorem elementwise, for all $\psi \in C_0^\infty(\Omega)$ we obtain

$$-\int_{\Omega} \nabla \psi \cdot \mathbf{w}_h dx = \int_{\Omega} \rho_h \psi dx - \sum_{T \in \mathcal{T}_h} \int_{\partial T} (\mathbf{w}_h \cdot \mathbf{n}_T) \psi ds.$$

Since the normal component of \mathbf{w}_h is continuous across interior edges and ψ vanishes on $\partial\Omega$, the boundary integral vanishes, and the lemma follows directly from the definition of weak divergence. \square

Previous work includes using $H(\text{div})$ -conforming HDG methods for the incompressible resistive MHD equations [7]. This class of methods notably streamlines computation in regions where system behavior is simpler and better understood. My choice of element is the Brezzi–Douglas–Marini (BDM) element, which is $H(\text{div})$ -conforming, suitable for problems that are highly flux-dependent, and largely compatible with hybridized methods. My proposed approach can be split into three stages: developing a formulation, verifying div-free condition, and evaluating performance against benchmarks. My immediate goal is to implement and validate a 2D div-free HDG solver and then extend my findings to 3D.

7 Conclusion

In this paper, I provided an overview of the ideal MHD equations and the numerical schemes commonly used to approximate their solutions. Finite difference methods offer a straightforward approach for constructing discrete approximations, while finite element methods provide a more flexible and stable framework for complex geometries. The eigenvalue formulation for plasma column stability illustrated how these numerical ideas appear in real physical modeling and how finite elements naturally arise.

Finally, I gave a brief overview of my proposed research directions, which focus on developing a div-free HDG method for coupled MHD–kinetic systems. The goal of this work is to improve shock capturing, reduce spurious oscillations, and ensure that important physical properties, such as magnetic flux conservation, are maintained. Numerical methods for plasma physics continue to present challenging and exciting problems.

8 Acknowledgments

I would like to thank Joe Denham for his mentorship with the Pitt–CMU Mathematics Directed Reading Program. I am also grateful to the program directors and to both the University of Pittsburgh and Carnegie Mellon University for supporting this project and giving me the opportunity to study Jardin’s *Computational Plasma Physics* in depth.

References

- [1] NASA, “Pulsed plasma rocket (ppr): Shielded, fast transits for humans to mars,” <https://www.nasa.gov/directorates/stmd/niac/niac-studies/pulsed-plasma-rocket-ppr-shielded-fast-transits-for-humans-to-mars/>, 2024, may 1, 2024; accessed December 7, 2025.
- [2] S. C. Jardin, *Computational Plasma Physics*. Springer, 2010.
- [3] Swiss Science Center Technorama, “light and sight” (licht und sicht) — exhibition,” <https://www.technorama.ch/en/scout/exhibitions/licht-und-sicht>, 2025, accessed December 7, 2025.
- [4] S. R. Wilson, “Nsf grfp research proposal: Divergence-free hdg methods for plasma modeling of mhd-kinetic systems,” 2025, unpublished proposal, submitted to the NSF Graduate Research Fellowship Program.
- [5] B. Ciucă *et al.*, “Implicit hybridized discontinuous galerkin methods for compressible magnetohydrodynamics,” *Journal of Computational Physics X*, vol. 5, p. 100042, 2019.
- [6] V. John, A. Linke, C. Merdon, M. Neilan, and L. G. Rebholz, “On the divergence constraint in mixed finite element methods for incompressible flows,” *SIAM Review*, vol. 59, no. 3, pp. 492–544, 2017.
- [7] Z. Chen, Z. Horváth, and T. Bui-Thanh, “A divergence-free and $h(\text{div})$ -conforming embedded-hybridized dg method for the incompressible resistive mhd equations,” *Computer Methods in Applied Mechanics and Engineering*, vol. 432, p. 117415, 2024.